On the Dependence of Materials Erosion on Environmental Parameters at Supersonic Velocities

George F. Schmitt, Jr.*
Wright-Patterson Air Force Base, Ohio

Investigation of the short exposure time rain erosion behavior of plastic, ceramic, metallic and composite materials at velocities of 1500 to 5500 fps has been accomplished using wedge and cone-shaped holders capable of exposing multiple materials samples at impact angles of 13.5°, 30°, 45° and 60° on the Holloman AFB, New Mexico rocket sled track. The erosion rate expressed as mean depth of penetration rate (MDPR) was found to vary with the square of the sine of the impact angle and 4.5 to 7 power of the velocity according to the following equation: MDPR = $KV^{\alpha} \sin^2 \theta$; where MDPR is mean depth of penetration rate, V is the velocity, K and α are constants for a particular material, and, θ is the impingement angle. A ($V \sin\theta$) term or normal component of the velocity governs the impact pressure up through 4000 fps at impingement angles of 30° or greater. However, at 5500 fps it was found that the tangential component of the velocity which influences the flow of an impinging water drop along the surface in a low angle (less than 30°), high velocity impact is as damaging as the impact pressure associated with the normal component of the velocity. This effect is highly significant for shallow angle cone shapes such as for high supersonic radomes and reentry vehicles.

Introduction

SUPERSONIC aircraft and missiles experience damage to radomes, leading edge surfaces, and structural members because of raindrop impingement. This phenomenon, known as rain erosion, has become increasingly severe as the velocity of these aerospace systems continues to increase.

The designers of radomes and aircraft have, in the past, relied on subsonic rotating arm erosion data extrapolated to higher velocities or on the qualification test of a mock-up radome by one firing through the rainfield on a rocket sled track. These investigations have been used to supposedly predict the behavior and performance of materials upon repeated exposure in a supersonic rain environment.

With the increasing numbers of supersonic aircraft and airborne missiles, a systematic comprehensive investigation of nonmetallic, dielectric materials, and metallic materials for structural applications was necessary to obtain erosion rates at supersonic velocities so that designers could develop efficient components which would withstand rain erosion under high speed, operational conditions.

The program as reported herein was directed toward obtaining these erosion rates as a function of velocity, angle of impingement, heating, rainfall intensity, and materials physical properties. Surface recession rates and weight loss per unit time were determined for materials which may be used in supersonic aircraft or missile systems.

Experimental

Rain erosion of ceramic, graphite, and plastic composite materials at high supersonic speeds has been extensively investigated by the Air Force Materials Laboratory over the past five years. Experimental evidence indicates that the coupled effects of aerodynamic heating and particulate erosion are severe with coupled damage increased by an order of magnitude over either heating or erosion alone. These in-house investigations were undertaken to determine the behavior of nonmetallic materials in a high supersonic rain environment (utilizing the Holloman AFB rocket sled track).

The rocket sled track at Holloman AFB is 35,500 ft long with 6000 ft equipped with rain nozzles (Spraying Systems Company Veejet 1/4 u 8070) mounted at 8 ft spacings on either side of the track but staggered so that there is a nozzle every 4 ft along the track. These nozzles were mounted at 65° from the horizontal and 31 in. above the track surface. At a pressure of 9 psi, they spray a cyclic fan-shaped pattern of droplets which then fall by gravity across the track with a mean drop size of 1.9 mm diam. A drop size distribution is shown in Fig. 4 (reproduced from Ref. 1). For the 4000 to 5500 fps tests, only 2000 ft of rainfield was used because of the severe damage at these high velocities. At velocities from 1500 fps to 4000 fps, the full 6000 ft was used. The rain density was 7.8 gs/m^3 for all tests.

The test program to date has consisted of supersonic exposures to rain of a variety of composite and bulk materials at Mach 1.5 to Mach 5.0 using four specially-designed fixtures which enabled multiple angle, multiple specimen experiments (see Figs. 1–3).

For runs up to Mach 4.0, two wedge-shaped holders which accommodated 80 and 48 −1.25 in. × 1.25 in. materials specimens respectively (16 each on the large wedge at 13.5, 30, 45, 60 and 90° and 12 each on the small wedge at 13.5, 30, 45 and 60°) were used. For the present tests at Mach 5.0, two right octagonal cones with half-angles of 13.5° (holding 32 specimens with 4 in each face) and 30° (holding 16 specimens with 2 in each face) were developed. These fixtures are mounted on the front of a rocket sled and by proper choice of rocket motors, various velocity profiles were achieved.

The wedge pictured in Fig. 1 was an adaptation of a larger wedge which was used for investigations up to Mach 3. To determine the droplet distortion and breakup characteristics because of the aerodynamic flow and shock wave effects, the shock wave patterns were photographed at all velocities of interest.

The shock wave patterns for the large and small wedges were photographed using Schlieren photography at all velocities of interest. The camera was mounted on a gantry above the track, and the photograph was taken vertically as the sled passed beneath the camera.

In Fig. 5 is a diagram of a typical shock pattern at Mach 2.5 on the wedge holder. Two major separated flow

Index Categories: Materials, Properties of; Structural Composite Materials (Including Loads); Hypervelocity Impact.

*Materials Engineer, Elastomers and Coatings Branch, Nonmetallic Materials Division of the Air Force Materials Laboratory. Members AIAA.

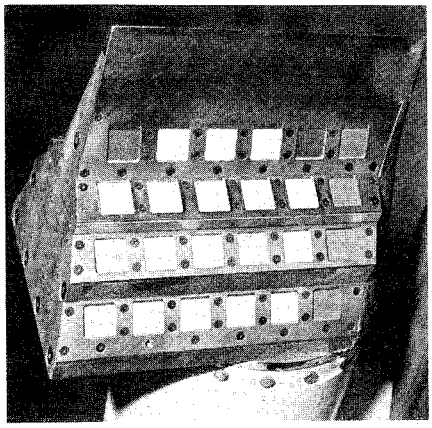

Fig. 1 Rain erosion wedge (4 angles).

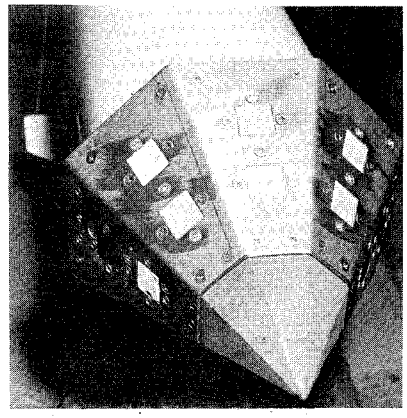

Fig. 3 Mach 5.0 30° rain erosion cone.

regions are indicated: one is in the corner between the 13.5 and 60° specimens; a second exists along the curved surface forward of the 90° specimen. Two minor separated flow regions are shown in the corners forward of the 45 and 30° surfaces. The interactions of these flow regions with the drops was found to be minor. As expected the shock pattern lays back closer to the wedge as the velocity increases.

The shock pattern for the small wedge at Mach 4 is similar to that of the large wedge indicated in Fig. 5 with the distances from the shock wave to the respective specimen positions correspondingly decreased over that at Mach 2.5.

Table 1 shows the path lengths, Δ_s, through which water drops must travel between penetration of the bow wave and impingement at the center of the specimen surfaces. These distances were determined by careful scaling from 16 × 20 in. blowups of the vertical Schlieren photographs.

The bow shock wave from the point of the wedge at supersonic speeds interacting with the water droplets can fragment them and thus affect the erosion results. While an aircraft designer would utilize such droplet-shock wave interactions as fully as possible to alleviate erosion effects, the assessment of materials erosion resistance at different angles of impingement requires as near a freestream condition as possible for all specimens.

Based upon vertical Schlieren photographs taken at each velocity at Holloman from which shock distances were scaled, the experimentally determined distances from shock to surface are plotted in Fig. 6.

Reinecke and Waldman[2] investigated the breakup of 2.12 mm diam droplets upon encounter with a normal incidence (90°) Mach 3 shock at 760 mm atmospheric pressures. They found that at a time of 150μ sec after shock encounter, the droplet mass was completely stripped away. This is exactly analogous to the conditions for the Mach 3 sled test. Based upon the measured distances from the shock to the specimen surfaces, the time available after shock encounter before striking the surface is 205 μsec at 90° indicating that drops of this size would be completely fragmented and no surface damage would occur. This has been borne out on the 90° data which was subsequently disregarded.

The Mach number corresponding to the component of velocity normal to the bow shock determines the time required for drop shattering by the air in the shock layer. The normal velocity components for the various specimen positions in the nominal Mach 3.0 run are 30°—1498 fps, 45°—2110 fps, 60°—2585 fps, and 13.5°—707 fps. For the other specimen positions at Mach 3, the times available for drop shattering to occur after shock encounter are 213 μsec at 30°, 98.7 μsec at 45°, 81.5° μsec at 60°, and 216 μsec at 13.5°, respectively. The Reinecke and Waldman experiments showed that at times of 80 μsec or less, 80% of the original mass was retained in the drop. Therefore, it appears that drops of 2 mm diam or less are significantly broken up prior to reaching the specimen surface except at 60°. However, the larger drops are less affected and, as can be seen by examining the droplet distribution

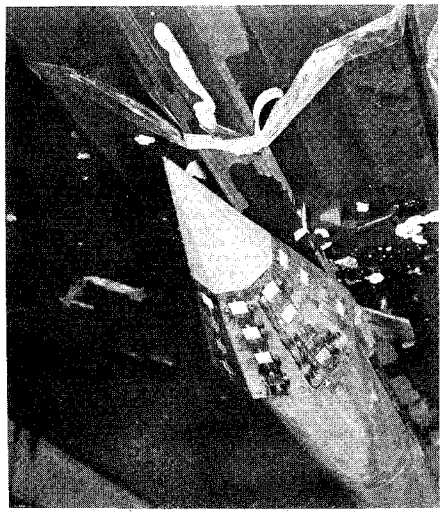

Fig. 2 Mach 5.0 13.5° rain erosion cone.

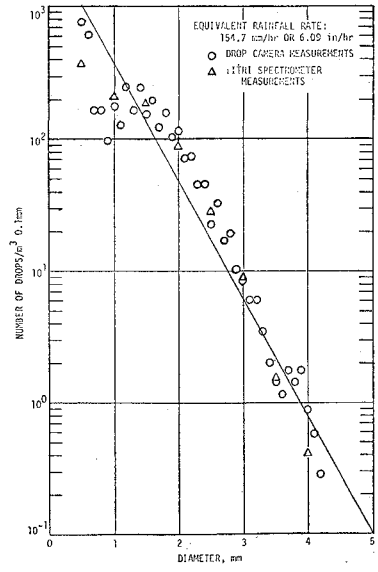

Fig. 4 Holloman rainfield drop size distribution.

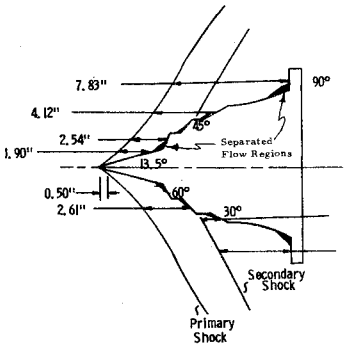

Fig. 5 Mach 2.5 shock pattern and distances.

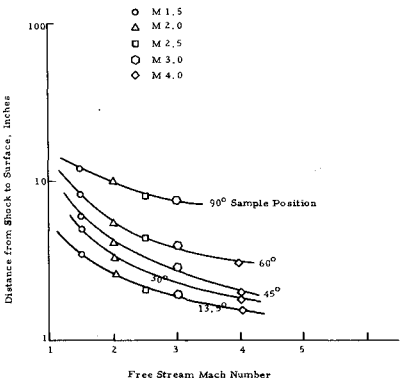

Fig. 6 Experimentally determined shock-to-specimen distances for rain erosion wedges.

in Fig. 4, tens of drops even if partially stripped, do strike the surface.

The principal goal of this research was the comparative behavior and relative ranking of advanced materials erosion resistance when exposed to identical supersonic rain environments.

The erosion rate-velocity-impingement angle dependence for the 13.5, 30, 45, and 60° specimens on both the large and small wedges and on the cones is also applicable to other flight cases as well. For example, the variation of erosion rate with impingement angle, the velocity exponents and the mass removal amounts, have been confirmed quantitatively in experiments on conical and sphere-cone ballistic range models in which bow shocks and uniform flow fields only existed around and in front of the materials.[3] The nonuniform flow field behind the bow shock in the wedge devices which did not exist behind the bow shock on the ballistics range models does not influence the erosion mass removal significantly in these tests. The effect of this complex flow field on the wedge devices should be to reduce the mass loss further and hence the values of mean-depth of penetration and mass loss are conservative.

Discussion

The determination of erosion rate-velocity dependence has long been a concern of investigators. In most investigations, including the one in this paper, the velocity is varied through a constant rainfield so that the rate of volumetric impingement increases directly as the velocity increases. The velocity exponent obviously will be one higher in this case than if it is based on constant rates of liquid impinging (only velocity changes). The discussion herein is directed toward the former situation.

Working with a constant rainfield, Fyall et al[4,5] have defined this dependence in terms of a threshold velocity

$$E_\alpha(V - V_c)^n \text{(usually } 3.5 < n < 3.6)$$

where E is the erosion rate based upon constant rainfall and V_c is a critical velocity value below which the material will not erode even at very long exposure times.

On the same basis, Hoff and coworkers[6] have preferred to define the erosion rate in terms of the absolute velocity

$$E_\alpha V^n \text{(usually } 4 < n < 6)$$

Hobbs[7] has concluded that at higher velocities based on constant rate of impinging liquid the erosion rate was found to increase with the fifth power of the velocity.

Heymann[8] has determined that the erosion rate based upon constant rate of liquid impinging will vary with the fifth power of the velocity. He arrives at the following expression by considering the damaging potential of the drop to be represented by the work done relative to the drop itself by the impact pressure. This work is proportional to the energy available in the high compressed drop to do damage by various mechanisms (impact, radial outflow, etc.) His expression is

$$R_e \alpha \left(\frac{\rho_0 C_0 V_0}{S}\right)^3 \left(\frac{V_0}{C_0}\right)^2$$

where R_e is "rationalized erosion rate" or volume of material eroded per unit time divided by volume of liquid impinged per unit time; ρ, C_0 are density and acoustic velocity of the liquid, V_0 is the normal impact velocity, and S is a strength property.

Thiruvengadam[9] has determined a fifth power variation for maximum erosion rate in low speed experiments through a constant rainfield on stainless steel and titanium.

It should be re-emphasized that the velocity exponents from the erosion rate (MDPR) analysis will be one greater than those obtained from a rationalized erosion rate. However, despite the different means of expressing this dependence, general agreement exists on the approximate

Table 1. Measured distances from shock wave to specimen positions of wedges

Velocity	Distance, in. 13.5°	60°	45°	30°	90°
Large wedge:					
Mach 1.5 (1702 fps)	3.44	5.14	6.10	8.08	12.11
Mach 2.0 (2372 fps)	2.50	3.175	3.93	5.30	9.67
Mach 2.5 (2671 fps)	1.90	2.54	2.61	4.12	7.83
Mach 3.0 (2996 fps)	1.88	2.53	2.74	3.82	7.38
Small wedge:					
Mach 4.0 (4644 fps)	1.82	1.74	2.02	3.28	None

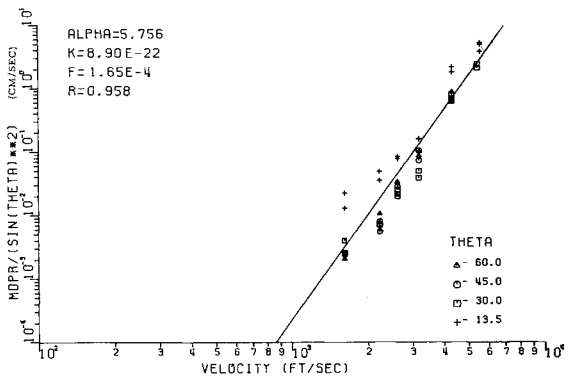

Fig. 7 Velocity-erosion rate dependence for PPO glass laminate.

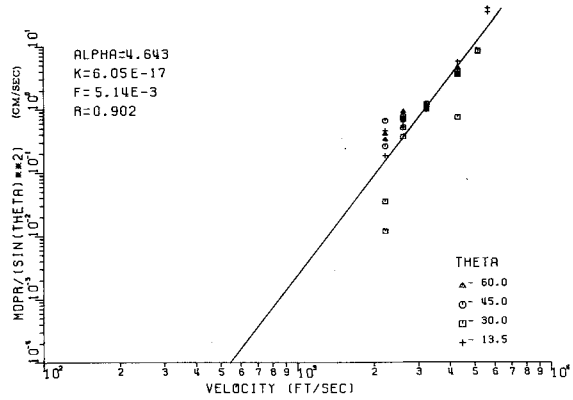

Fig. 8 Velocity-erosion rate dependence for isotropic pyrolytic boron nitride.

fifth power variation of rationalized erosion with the velocity.

Analysis and Results

In our analysis, a mean depth of penetration rate (cm/sec) has been defined in which edge effects or uneven erosion on the sample have been eliminated by assuming uniform erosion across the entire sample area. This MDPR is calculated from the weight loss, density, known surface area, and time of exposure as obtained from microsecond readings on the Holloman instrumentation.

A relationship was developed relating the mean depth of penetration rate (MDPR) as determined from the weight loss per unit area to the impact and the impingement angle θ, as follows: MDPR = $KV^{\alpha} \sin^2\theta$, where MDPR is mean depth of penetration rate, V is the velocity, K and α are constants for a particular material, and θ is the impingement angle.

The preceding expression with the $\sin^2\theta$ differs from our previously developed relationship[8]; viz

$$\text{MDPR} \sin\theta = K(V \sin\theta)^{\beta}$$

which correlated experimental data up through 4000 fps. The $V \sin\theta$ term or normal component of the velocity governs the impact pressure up through 4000 fps at impingement angles of 30° or greater. However, at 5500 fps it was found that the tangential component of the velocity which

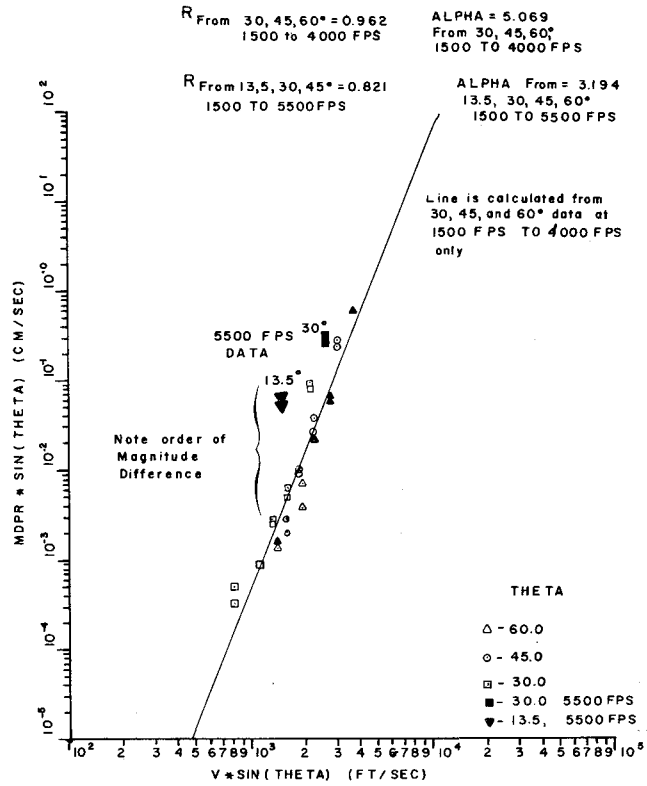

Fig. 9 Mean depth of penetration—normal velocity dependence for polyphenylene oxide-glass laminate.

influences the flow of an impinging water drop along the surface in a low angle (less than 30°), high velocity impact is as damaging as the impact pressure associated with the normal component of the velocity. This effect had not been isolated in any previous erosion investigations and is highly significant for shallow angle cone shapes at high supersonic velocities.

This investigation represents the only program which has examined materials rain erosion response at high supersonic speeds in a comprehensive manner. The investigation covers multiple rain particle impingement on specimens which are simultaneously heated aerodynamically and this coupled phenomena has been found to be quite significant.

Table 2. MDPR = $KV^{\alpha} \sin^2\theta$ rain erosion equation constants

Class	Material	α	K	r	No. of data pts
		Bulk ceramics			
A8	7941 Fused silica	4.480	9.22×10^{-17}	0.797	36
A13	Isotropic pyrolytic boron nitride	4.643	6.05×10^{-17}	0.902	28
A16	Silicon carbide (0.020″) on bulk graphite	5.243	1.11×10^{-19}	0.910	29
		Plastic laminates and composites			
C2	Furane B265 epoxy-glass	6.526	1.32×10^{-24}	0.981	32
C3	Epon 828 epoxy-glass	7.574	3.49×10^{-28}	0.970	41
C10	Polyphenylene oxide (531-801)-glass	5.756	8.90×10^{-22}	0.958	35
C13	Low void polyimide-glass	6.247	7.81×10^{-24}	0.956	25
M2	Perpendicular glass-epoxy composite	4.795	1.28×10^{-18}	0.863	19
I1	Polyphenylene oxide 531-801	8.721	9.80×10^{-33}	0.983	29
I2	Plexiglas (Type II-UVA)	6.402	5.54×10^{-24}	0.959	28
I3	Teflon (TFE)	4.642	1.13×10^{-17}	0.978	55

Among the important results from this investigation are:

a) The erosion rate (surface recession due to particle impingement) of composite materials varies with the fifth to 6.5 power of the velocity and the sine squared of the impact angle at speeds from 1500 to 5500 fps. This dependence is determined by computer analysis of weight loss data as a function of velocity and impingement angle. Computer-determined plots of mean-depth-of-penetration rate/$\sin^2\theta$ vs velocity are shown in Figs. 7 and 8. Values of velocity exponents, α, the value K in the equation, and the correlation coefficient, r, describing degree of fit for the various materials and the number of data points are tabulated in Table 2.

b) The failure of bulk brittle materials including dense ceramics such as alumina, beryllia and pyroceram and bulk graphites are the result of impact fracture. These materials do not erode as such. The erosion rate-velocity relationships for some isotropic ceramics could not be meaningfully developed because breakage of these materials under droplet impact was so severe that true erosion could not be measured. Only fused silica and isotropic pyrolytic boron nitride eroded rather than fractured and the erosion rate of these two ceramics varied with the 4.5 power of the velocity.

c) The coupled heating from the high-speed sled run and the erosion from rain droplets produces a high degree of charring and material removal of reinforced plastic composite materials, thus graphically demonstrating their limitations in this environment.

d) Reinforced laminates and composites cannot be used in an unprotected form because of their poor erosion resistance. The erosion of uncoated laminates was remarkably uniform and consistent. Heating effects at Mach 5 exert a considerable influence over the erosion behavior of polymeric-based materials as a function of their thermal stability. The low void polyimide glass laminate retains its strength better at elevated temperature and hence was less eroded than other laminates at 5000 fps. where thermal effects seriously degraded the epoxy-glass and polyphenylene oxide-glass laminates. However, all composites evaluated exhibited relatively poor erosion resistance and must be coated for erosion protection. The use of a three-dimensional fiber construction did not yield improved rain erosion resistance in a multiple particle environment compared to more conventional two-dimensional layups. A composite construction which incorporates the one dimensional orientation of fibers in the direction of the impinging drop exhibits potential for supersonic erosion resistance.

e) The tangential component of the velocity; that is, the component associated with flow of the droplet along the surface after impact, is significant at velocities of Mach 5 or above. The depth-of-penetration rate obtained for low angle (13.5°) exposures at Mach 5 is a full order of magnitude higher than that predicted from the normal velocity component and erosion rate-velocity dependence based upon supersonic speed relationships. This increased penetration is partially due to combined the thermal-particle erosion effects but its magnitude is much greater than would be predicted from higher angle, combined ablation-rain erosion data. This erosion effect is demonstrated in Fig. 9 where the relationship of the erosion at 13.5° and Mach 5.0 is shown with the other data from higher angle and/or lower velocity runs.

This finding is significant because no studies have been conducted at a combination of this high a velocity and this low an impingement angle before such that the tangential velocity component effect could have been determined.

The traditional technique for mitigating the damaging effects of erosion at high velocity has been to protect the 90° angle area with a metal/or ceramic tip and reduce the impingement angle to as low a value as possible consistent with transmission, drag and other requirements. The results of this high speed-low angle erosion investigation indicate that considerable damage can still occur in a supersonic rain exposure even at low angles.

In summary, the rain erosion response of advanced composite and bulk ceramic materials at velocities up to Mach 5 have been investigated and the coupled ablation-particle erosion is severe enough to seriously damage these materials at high impingement angles. The erosion rate of composite materials varies with the fifth to 6.5 power of the velocity and the sine squared of the impingement angle in the velocity range 1500 to 5500 fps. Ceramic and graphite materials fail as a result of impact fracture under these same conditions.

References

[1]Mueller, E. and Sims, A., "Measurement of the Simulated Rainfall at the Holloman Test Track Facility," AFCRL-70-0282, University of Illinois, Urbana, Ill., April 1970.

[2]Reinecke, W. G. and Waldman, G. D., "A Study of Drop Breakup Behind Strong Shocks with Applications to Flight," SAMSO-TR-70-142, Space and Missile Systems Organization, Los Angeles, Calif., May 1970.

[3]Reinecke, W. G., "Rain Erosion at High Speeds," submitted for AIAA 12th Aerospace Sciences Meeting, Washington, D.C., 30 January–1 February 1974.

[4]Fyall, A. A., King, R. B., and Strain, R. N. C., "Rain Erosion Aspects of Aircraft and Guided Missiles," *Journal Royal Aerospace Society*, Vol. 66, July 1962, pp. 447–453.

[5]King, R. B., "Multiple Impact Rain Erosion Studies at Velocities up to 450 m/s (M 1.3)," TR 67019, Jan. 1967, Royal Aircraft Establishment, Farnborough, England.

[6]Hoff, G., Langbein, G., and Rieger, H., "Material Destruction due to Liquid Impact," *Erosion by Cavitation or Impingement*, ASTM-STP 408, American Society for Testing and Materials, Philadelphia, Pa. 1967, pp. 42–69.

[7]Hobbs, J. M., "Factors Affecting Damage Caused by Liquid Impact," National Engineering Laboratory Rept. 262, Glasgow, Scotland, Dec. 1966.

[8]Heymann, F. J., "Toward Quantitative Prediction of Liquid Impact Erosion," *Characterization and Determination of Erosion Resistance*, ASTM-STP 474, American Society for Testing and Materials, Philadelphia, Pa., 1970, pp. 212–248.

[9]Thiruvengadam, A. and Rudy, S. L., "Experimental and Analytical Investigations on Multiple Liquid Impact Erosion," TR 719/1, National Aeronautics and Space Administration Contract NASW-1608, June 1968, Hydronautics, Inc., Laurel, Maryland.

[10]Schmitt, G. F., Jr., "Erosion Rate-Velocity Dependence for Materials at Supersonic Speeds," *Characterization and Determination of Erosion Resistance*, ASTM-STP-474, American Society for Testing and Materials, Philadelphia, Pa., 1970, pp. 323–352.